NASA Technical Memorandum 101379
AIAA-89-0565

Control of "Laminar Separation" Over Airfoils by Acoustic Excitation

K.B.M.Q. Zaman and D.J. McKinzie
Lewis Research Center
Cleveland, Ohio

(NASA-TM-101379) CONTROL OF LAMINAR SEPARATION OVER AIRFOILS BY ACOUSTIC EXCITATION (NASA) 19 p CSCL 01A

N89-12552

Unclas
G3/02 0174546

Prepared for the
27th Aerospace Sciences Meeting
sponsored by the American Institute of Aeronautics and Astronautics
Reno, Nevada, January 9-12, 1989

CONTROL OF "LAMINAR SEPARATION" OVER AIRFOILS BY ACOUSTIC EXCITATION

K.B.M.Q. Zaman and D.J. McKinzie
NASA Lewis Research Center
Cleveland, Ohio 44135

E-4434

Abstract

The effect of acoustic excitation in reducing "laminar separation" over two-dimensional airfoils at low angles of attack is investigated experimentally. Airfoils of two different cross sections, each with two different chord lengths, are studied in the chord Reynolds number range of 25 000 < R_c < 100 000. While keeping the amplitude of the excitation induced velocity perturbation a constant, it is found that the most effective frequency scales as $U_\infty^{3/2}$. The parameter $St/R_c^{1/2}$, corresponding to the most effective f_p for all the cases studied, falls in the range of 0.02 to 0.03, St being the Strouhal number based on the chord.

Nomenclature

α	angle of attack
C_l	lift coefficient
c	chord of airfoil
f_{mn}	tunnel cross resonance frequency with m sound pressure nodes in y, and n sound pressure nodes in z
f_p	excitation frequency
L_r	sound pressure level at reference microphone location
R_c	chord Reynolds number
St	Strouhal number, $f_p c/U_\infty$
U,V	mean velocities in x,y directions, respectively
$\langle U \rangle$	mean velocity measured with a single hot wire approximating $(U^2 + V^2)^{1/2}$
U_∞	freestream U
u',v',w'	rms velocity fluctuations in x,y,z directions; subscript r denotes values at reference location
$\langle u' \rangle(f)$	one-dimensional spectrum of $\langle u' \rangle$
$\langle u' \rangle, \langle u'_f \rangle$	rms total and fundamental fluctuation in the direction of $\langle U \rangle$, as measured by a single hot wire
$\langle u'_r \rangle$	$(u_r'^2 + v_r'^2)^{1/2}$
x'	streamwise distance from leading edge
x,y,z	streamwise, transverse, and spanwise coordinates

Introduction

Several experiments have demonstrated that artificial excitation can reduce the tendency towards separation in the flow over an airfoil and thereby improve its performance.[1-7] The separation process, and the effect of excitation thereupon, has been noted to be different depending on the ranges of the angle of attack and the Reynolds number.[5] While at all R_c the flow separates ultimately at large α (poststall), an unsteady separation may occur around the static stall condition.[5,8] At sufficiently low R_c, on the other hand, extensive separation on the suction side may take place even at low α. This is accompanied by a rapid deterioration of the airfoil performance with decreasing R_c, approximately in the range R_c < 100 000.

The low α separation at R_c = 40 000 is illustrated in Fig. 1 by visualization pictures taken from Ref. 5. Note that the flow on the upper surface is separated for all the lower α's but has reattached at the highest α, presumably due to earlier transition of the separated shear layer in that condition. Stability analysis, carried out in Ref. 5, indicated that the boundary layer prior to separation for the low α cases must be stable and thus laminar. The flow separation at the low α and low R_c is simply referred to in the following as "laminar separation". The effect of excitation on this separation is the focus of the present study.

In the references cited above, the effect of artificial excitation has been studied mostly for poststall conditions. References 2, 3, and 5 provided some data showing that acoustic excitation can also reduce the extent of the laminar separation. However, the excitation data in all previous studies covered only limited parametric ranges. Much of the data were of demonstration type and insufficient to address the scaling of the effective excitation parameters in any of the situations described above.

The purpose of the present experiment is to gain a better understanding of the excitation effect, specifically focusing on the laminar separation. The principal objective is to determine the envelopes of excitation frequencies effectively reducing the separation. The experiment is designed to cover a wide excitation frequency range, and the available parametric ranges are explored systematically. Airfoils of two different cross-sectional shapes having different stalling characteristics, each with two different chords, are tested. The tunnel resonant frequencies, as will be addressed further, are given reasonable consideration. The effect on the lift coefficient is used as the primary diagnostic for assessing the influence of the excitation. The scaling of the effective frequency envelopes is then analyzed. Details of the flow field for a specific excitation case are also studied in comparison with the corresponding unexcited flow field.

Experimental Facility

The experiments are carried out in the NASA Lewis Low Speed Wind Tunnel, which has been described in detail elsewhere.[8] It has a test section with 76- by 51-cm cross section. The freestream turbulence intensity is less than 0.1 percent. Two-dimensional models of a LRN-(1)-1007 and a Wortmann FX 63-137 airfoils are used.[8] For each type, two models with chords 12.7 and 25.4 cm are employed. The airfoils are supported at midchord and span the entire test section. Figure 2(a) is a photograph of the test section fitted with the c = 12.7 cm LRN airfoil.

A schematic of the test section is shown in Fig. 2(b). Two acoustic drivers (Altec Lansing 291-16K; rated 0.5 to 20 kHz) and a 40.6 cm woofer (Altec Lansing 515-8G; rated 40 Hz to 4 kHz) were mounted on the ceiling. Even though the amplitude fell off, the woofer could be used for excitation at f_p as low as 15 Hz. The sound from the woofer entered the test section through a 30.5 cm diameter opening. The opening was covered with a 64-mesh screen. The sound from the acoustic drivers entered the test section via 3.8 cm holes in the ceiling. For all data presented, only one speaker was used at a time; for $f_p < 700$ Hz the woofer was used, for $f_p > 700$ Hz one of the acoustic drivers was used.

A 1/4-in (B & K) microphone, flush mounted on the ceiling, was used to measure a reference sound pressure level (L_r). A crossed hot-film probe (DISA 55R53) was used to measure velocity fluctuation amplitudes (u' and v'). The probe, at the reference location, can be seen in Fig. 2(a). The DISA 55R53 probe was replaced by a DISA 55R54 probe to measure w'. A computer controlled traversing mechanism was used to move a single hot wire to measure the velocity field around the airfoil. The coordinate origin is at the tunnel midheight ($y = 0$) and midspan ($z = 0$) and at the airfoil support at midchord ($x = 0$). For convenience, the streamwise coordinate (x') for some data has been referenced to the airfoil leading edge.

Results and Discussion

C_l versus α for the c = 12.7 cm LRN airfoil is shown in Fig. 3(a) for various R_c. The cross section of the airfoil is shown by the inset in the figure. Note that the curves are staggered. For $R_c \geq 35\,000$, the C_l curves are marked by a "sag" at low α.[2] This is due to the laminar separation. Note that at relatively higher α, the airfoil recovers to the high lift condition due to reattachment of the flow occurring naturally (Fig. 1). This occurs presumably due to the earlier transition of the separated shear layer at the higher α; the exact mechanism remains unclear. Note that the sag in the C_l curve becomes more pronounced at lower R_c. At $R_c = 25\,000$, the flow remains separated throughout the α range, and the airfoil completely loses its efficiency in producing high lift.

Essentially the same behavior is observed with the Wortmann airfoil (Fig. 3(b)). Note that complete separation commences at $R_c = 50\,000$ in this case. Another difference is in the stall characteristics. The Wortmann clearly shows stall hysteresis while the LRN does not in the same wind tunnel environment. The Wortmann airfoil is of the "leading edge stall" type whereas the LRN airfoil is approximately of the "trailing edge stall" type.[8] In the following, attention is focussed on the laminar separation at low α; <u>all subsequent data are for $\alpha = 6°$.</u>

Figure 4 shows the Reynolds number effect on C_l of the two airfoils. Clearly, laminar separation persists up to $R_c \approx 60\,000$ for the LRN airfoil, and up to $R_c \approx 75\,000$ for the Wortmann airfoil. While these data are for the c = 12.7 cm models, the jump to the higher C_l occurred at somewhat higher R_c with the c = 25.4 cm models. Note that the jump in the C_l, associated with the elimination of the laminar separation, does not involve hysteresis even for the Wortmann airfoil.

The tunnel resonance characteristics were documented by measuring the reference velocity and sound pressure amplitudes while exciting the flow with the loudspeakers. The LRN airfoil at $\alpha = 6°$ was in the flow with $R_c = 50\,000$. The woofer was used for $f_p < 700$ Hz and one acoustic driver for $f_p > 700$ Hz. The input voltage to each speaker was held constant. L_r and the reference velocity amplitudes were measured while f_p was varied in discrete steps. These data are shown in Fig. 5.

The u_r' data show that longitudinal resonances are set up at the lower end of the f_p range covered. The 23 Hz peak ought to correspond to half wave resonance involving the entire length of the tunnel. The 59 Hz peak must be the half wave resonance corresponding to the length of the test section on either end of which the cross-sectional area diverges. Resonances at several higher harmonics of 59 Hz also occur in the u_r' data. Note that the induced v_r' and w_r' at these lower f_p's are essentially equal to the freestream amplitudes. The freestream amplitudes (without excitation) have been shown at 10 Hz; these amplitudes are somewhat overestimated due to noise from the anemometer circuitry.

The fundamental cross resonance in the y direction occurs around 342 Hz. Note that v_r' is very large at this frequency, but u_r' is practically zero. (Thus, a single hot wire at the reference location would fail to sense this resonance.) Several peaks occur in the v_r' data, notably at 570 Hz, 995 Hz, 1400 Hz, etc. The frequencies of the cross resonances at low Mach number are given by:[9,10]

$$f_{mn} = \frac{a_0}{2\left[(m/H)^2 + (n/W)^2\right]^{1/2}}$$

where m and n are integers, H and W are the height and the width of the test section, respectively, and a_0 the speed of sound.

Note that with the given orientation of the loudspeakers, little w_r' fluctuation is induced. The woofer fails to excite the fundamental cross resonance in the z direction, which if induced should have marked the w_r' data by a peak around 224 Hz. Note also that for constant voltage input to the speakers the SPL, L_r, is strongly affected by especially the cross resonances. Here, let us mention that data similar to those in Fig. 5 were also obtained in the empty tunnel with the airfoil taken out but with all other conditions remaining constant. Essentially similar variations for the major resonance peaks were observed, except that the amplitudes were somewhat lower.

The u' and v' amplitudes were measured as a function of y (with the airfoil in), at $z = 0$ and the reference x location, for a few resonant frequencies. These are shown in Fig. 6(a). Corresponding spanwise variations of the amplitudes, at the reference x and y, are shown in Fig. 6(b). These data indicate that the u' amplitude at 59 Hz is approximately constant over the entire cross section. Data at a few other low f_p's (<280 Hz, not shown) also showed similar uniform amplitudes.

For $f_p = 342$ Hz and higher the v' data exhibit expected nodal patterns, which can also be used to identify the specific cross resonance modes. Thus, the frequencies 342, 570, and 688 Hz can be identified as the f_{10}, f_{12}, and f_{20} modes, respectively. 995 Hz appears to correspond to the f_{33} mode from the v' distribution, but the frequency computed from the equation of f_{mn} differs significantly. The difference remains unexplained; however, one should note that the tunnel conditions are different from those of an idealized resonating duct, especially in view of the presence of the airfoil.

The excitation amplitude effect on various parameters is documented in Fig. 7(a). C_l versus L_r data are shown in the bottom graph. For the flow under consideration, the most pronounced effect on C_l occurs in the f_p range of 116 to 342 Hz. Corresponding variations in u_r' and v_r' with L_r are shown on the top of Fig. 7(a). Note that at 116 and 253 Hz, u_r' is large and v_r' is essentially zero while the reverse is true for 342 Hz. Yet the flow is influenced at either frequency in a consistent pattern. This indicates that inducing either velocity component upstream of the leading edge is equally effective in the excitation of the flow.

Referring back to Figs. 5 and 6, note that for a given f_p either u_r' is large and v_r' is small or vice versa. In the study of excitation frequency effect, it was desirable to keep a particular component of the velocity amplitude in the incoming flow a constant. However, because of the resonances it would be impossible to achieve that in a wind tunnel. Since inducing either u_r' or v_r' seemed to have the same effect, it was decided that the resultant $\langle u_r' \rangle = (u_r'^2 + v_r'^2)^{1/2}$ would be kept constant for the subsequent data. For the lower f_p's (<280 Hz), this reasonably approximated the condition where u_r' was held constant in the incoming flow over the entire tunnel cross section. For the specific modes like f_{10} (=342 Hz), f_{30} (≈1026 Hz), etc., this approximated a constant v_r' near the leading edge over the entire span of the airfoil. At other f_p's the amplitude can be expected to be nonuniform along the span. However, it should be obvious that $\langle u_r' \rangle$ at the chosen reference location should be a much more meaningful amplitude parameter than a velocity amplitude elsewhere or the SPL anywhere in the tunnel.[5,6]

C_l versus $\langle u_r' \rangle$ are cross plotted in Fig. 7(b) from the data of Fig. 7(a). It is clear that around the "effective" frequency it takes a small amplitude to reattach the flow yielding the higher lift. The curves are seen to flatten out with increasing $\langle u_r' \rangle$, indicating that the flow has reattached optimally at the low amplitudes leaving no room for further improvement.

The excitation frequency effect, with the amplitude $\langle u_r' \rangle / U_\infty = 0.5$ percent held constant, is shown in Fig. 8(a) for the LRN airfoil. For the chosen amplitude, spectral analysis of u_r' and v_r' for several f_p's indicated "pure tone" excitation; higher harmonics in the worst cases were no larger than 2 percent of the fundamental in rms amplitude. The data are shown from the lowest R_c, where C_l could yet be resolved reliably with the given instrumentation, to the highest R_c above which the flow reattached naturally. Note that there are data from airfoils of two different chords. Clearly, the effective f_p range increased and shifted to the right with increasing R_c for a given airfoil.

Figures 8(b), (c), and (d) are cross plots of the data of Fig. 8(a) as a function of the indicated abscissae. Inspection of these figures should convince one that the parameter $St/R_c^{1/2}$ best aligns the effective f_p bands. The same inference can be reached from the corresponding data for the Wortmann airfoil, shown similarly in Figs. 9(a) to (d). It is remarkable that a nondimensional parameter has emerged out of this exercise, at a given value of which, viz. at $St/R_c^{1/2} \approx 0.025$, the excitation is most effective for airfoils of two different cross sections each with two different chords.

The flow at $R_c = 50\,000$ with the $c = 12.7$ cm LRN airfoil at $\alpha = 6°$ was chosen for detailed flow field measurements with and without excitation. The excitation was at 253 Hz corresponding to $St/R_c^{1/2} = 0.025$. Some of these data were obtained at an earlier time when the $\langle u'_r \rangle$ amplitude was not measured. It is estimated to be about 0.25 percent of U_∞ for these cases. However, Fig. 7(b) indicates that the difference in the amplitudes should not make significant difference in the overall flow fields.

Figure 10 shows the distribution of "$\langle U \rangle$-extrema", around the airfoil, as explained in the following. These data were obtained by traversing a single hot wire (sensing the resultant of U and V, which is denoted as $\langle U \rangle$). At a given x' on the upper surface, $\langle U \rangle$ was maximum near but outside the boundary layer, and decreased slowly with increasing distance away from the airfoil surface. Underneath the airfoil, the velocity outside the boundary layer was lower than U_∞ and slowly increased away from the airfoil. At $\alpha = 6°$, the rate of change of $\langle U \rangle$ with y was slow, and thus, traversing the hot wire at constant y near the airfoil reasonably captured the distribution of $\langle U \rangle$ values that would be expected just outside the boundary layer. The data of Fig. 10 were measured accordingly. Thus, these data approximate the "potential flow" velocity distribution and can provide an estimate of the C_p distribution around the airfoil, C_p being the pressure coefficient. Note that the excitation enlarges the area under the $\langle U \rangle$ envelope, and hence under the C_p envelope, commensurate with the increased lift obtained with the excitation. $(\delta\langle U \rangle / \delta x) \cdot (c/U_\infty)$ is found to be about 0.3 around 30 percent chord location. The corresponding value of $\delta Cp/\delta(x/c)$ turns out to be about 0.78.

Figure 11 shows the boundary layer mean velocity (⟨U⟩) profiles at various streamwise locations on the upper surface of the airfoil. Note that the curves are staggered laterally, but for each x', the pair of profiles with and without excitation are shown with the same scale. For each profile, the bottom most data indicate the location of the airfoil surface. Note also that near the surface the measurements are erroneous due to hot-wire rectification during flow reversal in the separated flows. Nevertheless the measured profiles provide an indication of the size of the separated regions. The flat segments in the profiles, prior to the increase in ⟨U⟩ with increasing y, should correspond to the separated regions. Clearly, the excitation reduces the size of the latter, and reattachment is achieved up to about 50 percent chord location. However, it is clear that for this case complete reattachment has not occurred and there exists a separated region even with the excitation.

Estimates of the boundary layer momentum thickness, θ, were obtained from these data. The integration was truncated at the point where ⟨U⟩ was 20 percent of local ⟨U⟩ maximum, to avoid contribution from the erroneous data in the separated region. The integration was truncated on the other end at 95 percent ⟨U⟩ maximum point. (Note that this way θ is reasonably measured in the boundary layer at the upstream locations; however, it is underestimated for the separated shear layer as the momentum defect in the reversed flow is not taken into account.) θ (mm) for three x locations are listed below. The Reynolds number and the Strouhal number of excitation, based on θ at $x'/c = 0.3$, for the unexcited flow, turn out to be 79 and 0.012, respectively.

x'/c	θ, Unexcited	θ, Excited
0.3	0.2	0.28
0.5	0.27	0.28
0.7	0.47	0.47

The fluctuation intensity profiles in the boundary layer corresponding to the data of Fig. 11 are shown in Fig. 12. Note that with the excitation the total fluctuation intensity is reduced somewhat at all stations. The fundamental amplitudes show that the instability wave, for the case documented, grows perceptibly beyond 50 percent chord location (discussed further in the following).

Figure 13 shows the ⟨u'⟩ spectra in the boundary layer at transverse locations where ⟨U⟩ is 70 percent of the local ⟨U⟩ maximum. At this transverse location the fundamental fluctuation intensity is approximately the maximum. It is apparent that the amplitude of the peak at 253 Hz (⟨u'_f⟩) starts growing substantially beyond the 50 percent chord location. At 80 percent chord location, the evolution of a subharmonic is apparent (dashed curve). Further downstream the spectral peaks are lost beneath the broadband turbulence. It is also evident that the effective excitation frequency closely matches the natural instability in the corresponding unexcited flow as apparent from the pairs of spectra at 60 and 70 percent chord locations.

The fundamental amplitude growth along the 70 percent velocity point was measured for three f_p, and are shown in Fig. 14. The inset shows variations of the amplitudes upstream, not covered in the main figure, but along a constant height (y) passing through the 70 percent velocity point at $x'/c = 0.2$. Note that the reference amplitude ⟨u'_r⟩ was held constant at 0.5 percent of U_∞. However, at 342 Hz, only v' is induced upstream of the leading edge, u' being very small. Thus, the measured amplitude ⟨u'_f⟩ there is small since the single hot wire primarily senses the amplitude in the direction of the mean flow. As the leading edge of the airfoil is approached u' for 342 Hz becomes large, even larger than the amplitudes for the other two f_p's.

Downstream of the leading edge the amplitude variations show standing wave patterns, reminiscent of the acoustically excited boundary layer data of Ref. 11. This occurs due to the interference of the excited instability wave and the exciting acoustic wave when the amplitudes due to the two are comparable. The wavelength of the standing wave should exactly equal the shorter hydrodynamic (instability) wavelength (λ). λ for the three f_p's were obtained from Fig. 14; λ and f_p provided the phase velocity of the instability wave. These quantities and the Strouhal number based on θ at $x'/c = 0.3$ are listed below.

f_p	λ/c	$\lambda f_p/U_\infty$	$f_p\theta/U_\infty$
168	0.14	0.51	0.008
253	0.10	0.55	0.012
342	0.077	0.57	0.016

Further downstream, one observes that the amplitude at 168 Hz grows to the largest value. This appears anomalous as, referring back to Fig. 8, 253 Hz is found to be the center frequency in the band of effective f_p's. Thus, intuitively one would expect a larger amplitude growth at 253 Hz. The reason for this remains unclear, but differences in the tunnel resonance conditions could be a contributing factor. One also notes from Fig. 14 that the amplitudes rise sharply for all f_p's past the 50 percent chord location. Referring back to the boundary layer profiles in Fig. 11, it is apparent that the amplification of the imposed disturbance takes place in the separated shear layer.

Conclusion

Small amplitude acoustic excitation at an appropriate frequency can effectively reduce laminar separation occurring on the suction side of airfoils at low α and low R_c. This results in a significant improvement in the lift coefficient. It is inferred from data with airfoils of two cross-sectional shapes, each with two different chords, that the optimum effect occurs when the parameter $St/R_c^{1/2}$, corresponding to the excitation frequency, falls in the range of 0.02 to 0.03. Detailed flow field data recorded for a specific case, indicate that a separated region still exists under the excitation, and the amplification of the imposed perturbation takes place primarily in the downstream shear layer rather than in the upstream boundary layer.

References

1. Collins, F.G. and Zelenevitz, J., "Influence of Sound Upon Separated Flow Over Wings," AIAA Journal, Vol. 13, No. 3, Mar. 1975, pp. 408-410.

2. Carmichael, B.H., "Low Reynolds Number Airfoil Survey: Vol. I," NASA CR-165803, 1981.

3. Mueller, T.J. and Batill, S.M., "Experimental Studies of Separation on a Two-Dimensional Airfoil at Low Reynolds Numbers," AIAA Journal, Vol. 20, No. 4, Apr. 1982, pp. 457-463.

4. Ahuja, K.K. and Burrin, R.H., "Control of Flow Separation by Sound," AIAA Paper 84-2298, Oct. 1984.

5. Zaman, K.B.M.Q., Bar-Sever, A., and Mangalam, S.M., "Effect of Acoustic Excitation on the Flow Over a Low-Re Airfoil," Journal of Fluid Mechanics, Vol. 182, Sept. 1987, pp. 127-148.

6. Neuburger, D. and Wygnanski, I., "The Use of a Vibrating Ribbon to Delay Separation on Two-Dimensional Airfoils: Some Preliminary Observations," Workshop on Unsteady Separated Flow, Air Force Academy, July 1987 (private communication).

7. Huang, L.S., Maestrello, L., and Bryant, T.D., "Separation Control Over an Airfoil at High Angles of Attack by Sound Emanating From the Surface," AIAA Paper 87-1261, June 1987.

8. Zaman, K.B.M.Q., McKinzie, D.J., and Rumsey, C.L., "A Natural Low Frequency Oscillation of the Flow Over an Airfoil Near Stalling Conditions," Journal of Fluid Mechanics, 1988 (submitted). (NASA TM-100213.)

9. Goldstein, M.E., Aeroacoustics, McGraw-Hill, 1976.

10. Baumeister, K.J., "Reverberation Effects on Directionality and Response of Stationary Monopole and Dipole Sources in a Wind Tunnel," Journal of Vibration, Acoustics, Stress, and Reliability in Design, Vol. 108, No. 1, Jan. 1986, pp. 82-90.

11. Leehey, P. and Shapiro, P., "Leading Edge Effect in Laminar Boundary Layer Excitation by Sound," Laminar Turbulent Transition, R. Eppler and H. Fasel, eds., Springer-Verlag, New York, 1979, pp. 321-331.

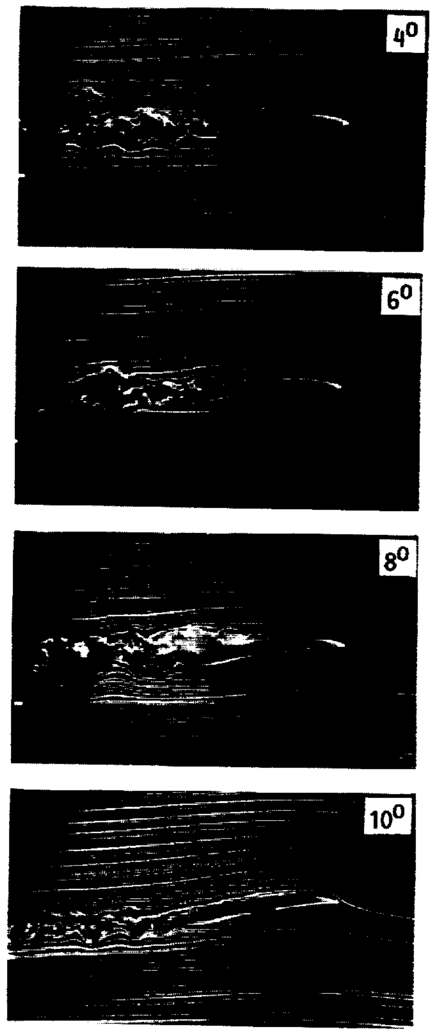

FIG. 1 - SMOKE-WIRE FLOW VISUALIZATION PICTURES FOR VARIOUS α FOR LRN AIRFOIL (c = 10.2 CM) AT $R_c = 4 \times 10^4$, REF. [5].

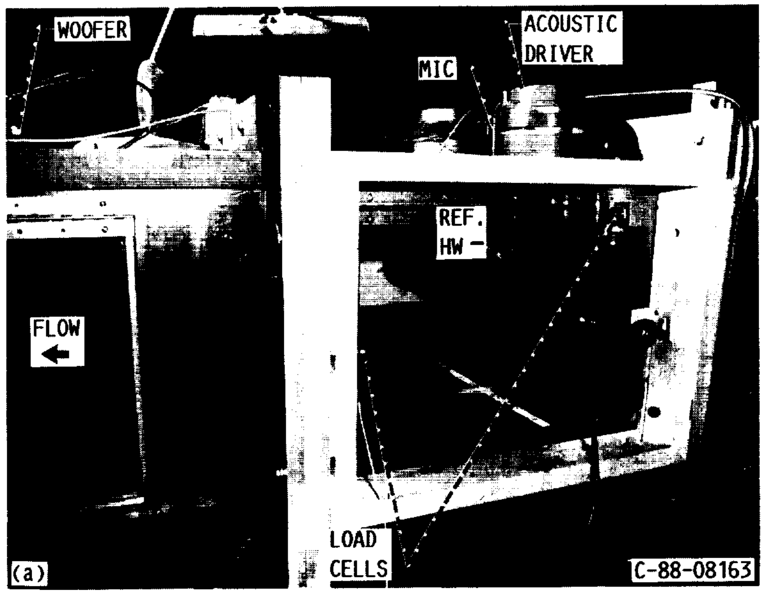

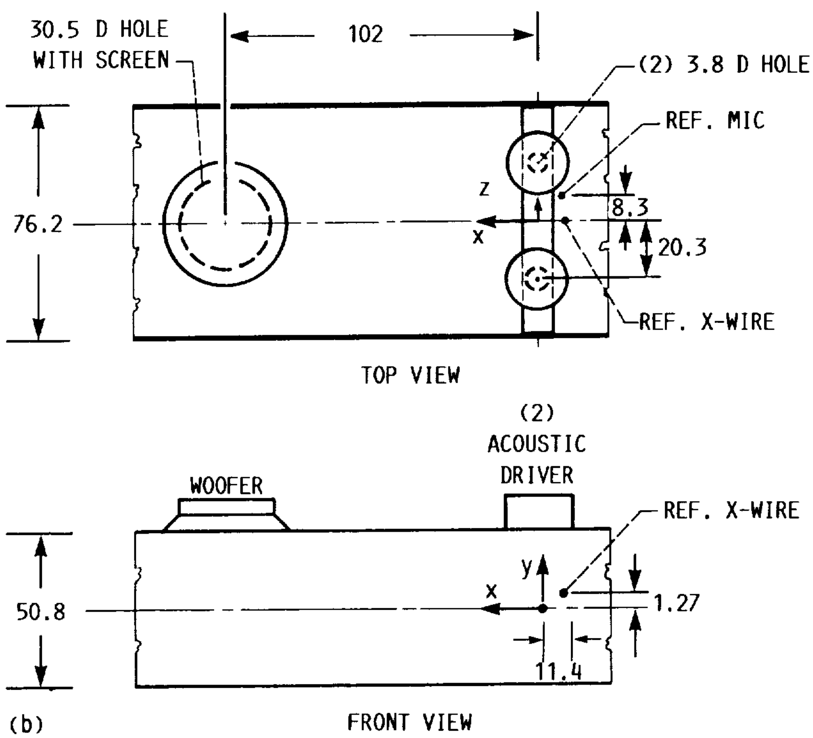

FIG. 2(a) - PHOTOGRAPH OF WIND TUNNEL TEST SECTION. (b) - SCHEMATIC OF TEST SECTION; DIMENSIONS ARE IN CENTIMETERS.

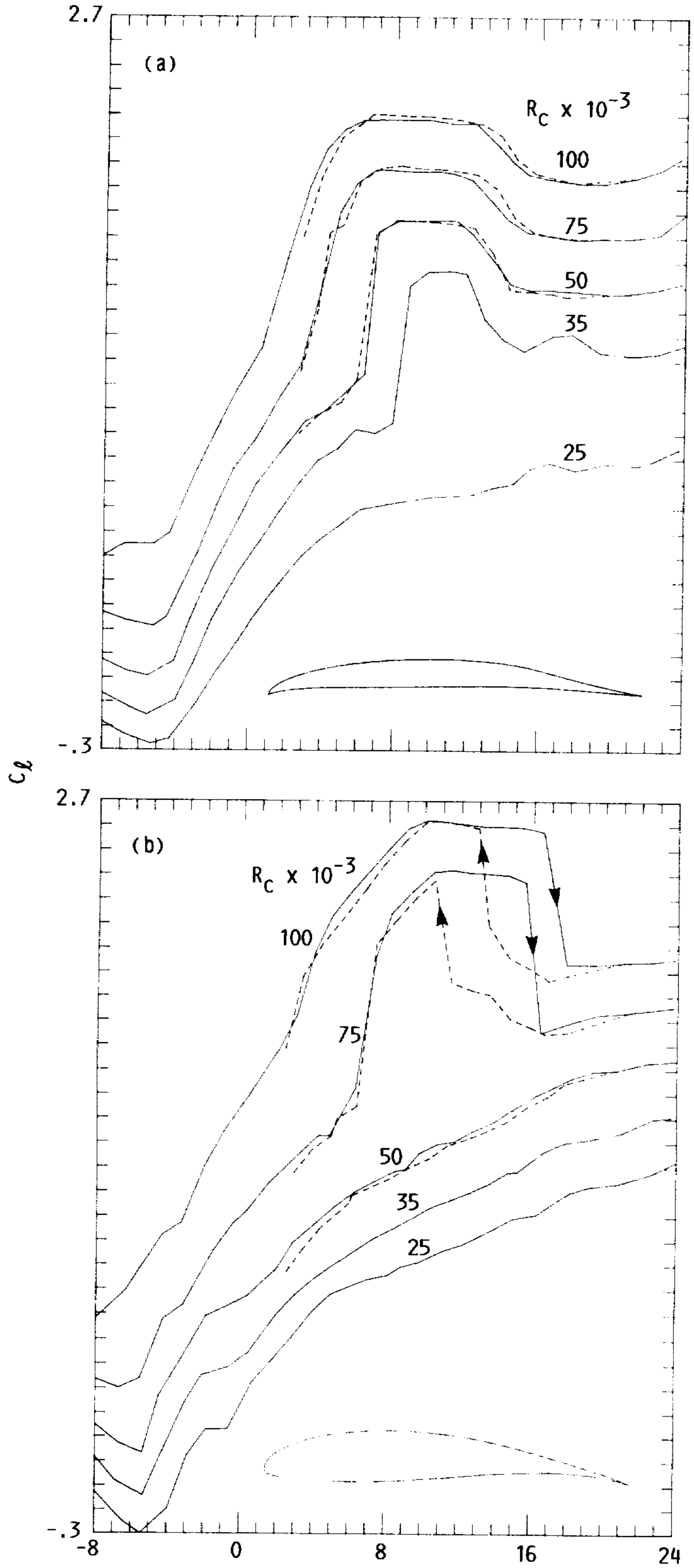

FIG. 3(a) - C_1 VERSUS α FOR c = 12.7 CM LRN AIRFOIL AT VARIOUS R_c. ORDINATE APPLIES TO BOTTOM CURVE, OTHERS ARE STAGGERED SUCCESSIVELY BY ONE DIVISION. SOLID CURVES FOR INCREASING α, DASHED CURVES FOR DECREASING α. (b) - C_1 VERSUS α FOR c = 12.7 CM WORTMANN AIRFOIL.

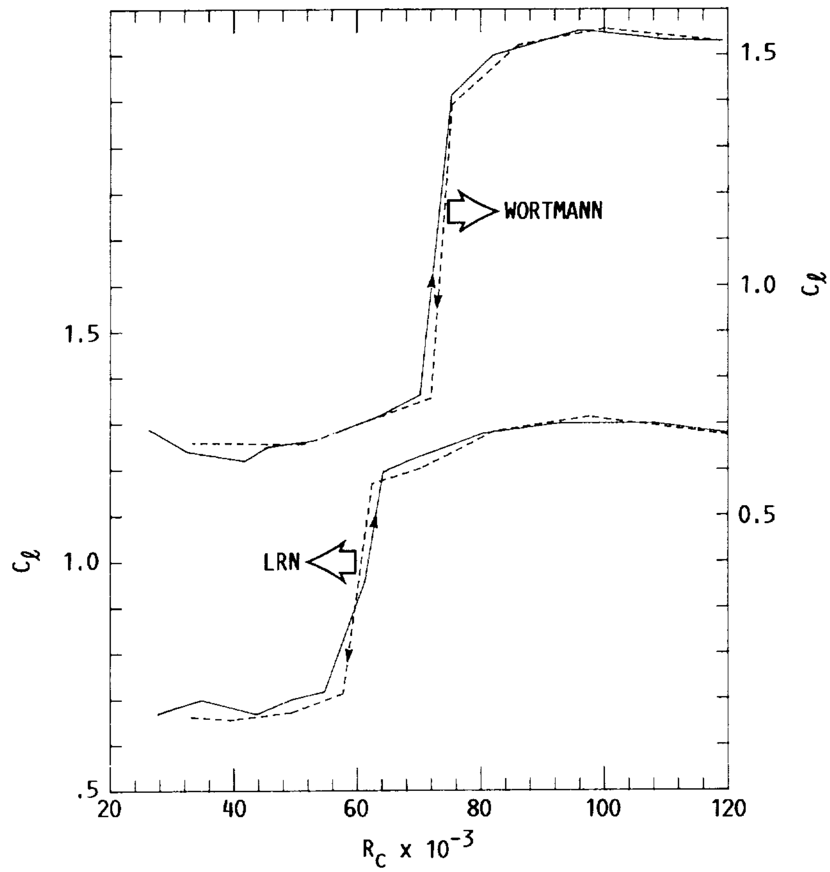

FIG. 4 - C_1 VERSUS R_c AT $\alpha = 6^0$ FOR THE TWO AIRFOILS; c = 12.7 CM.

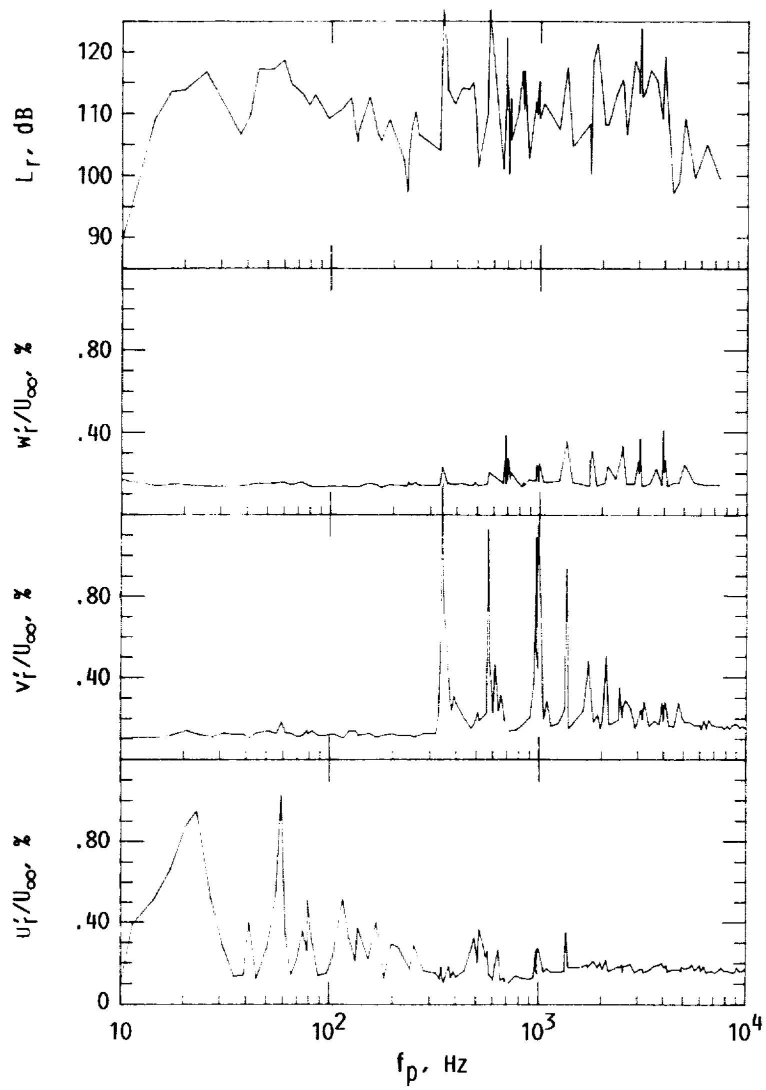

FIG. 5 - REFERENCE AMPLITUDE PARAMETERS VERSUS f_p. HOT-WIRE AT $x = -11.4$ CM, $y = 1.27$ CM, AND $z = 0$; MICROPHONE LOCATED AS SHOWN IN FIG. 2(b). $c = 12.7$ CM LRN AIRFOIL AT $\alpha = 6^0$ WITH $R_c = 50\ 000$.

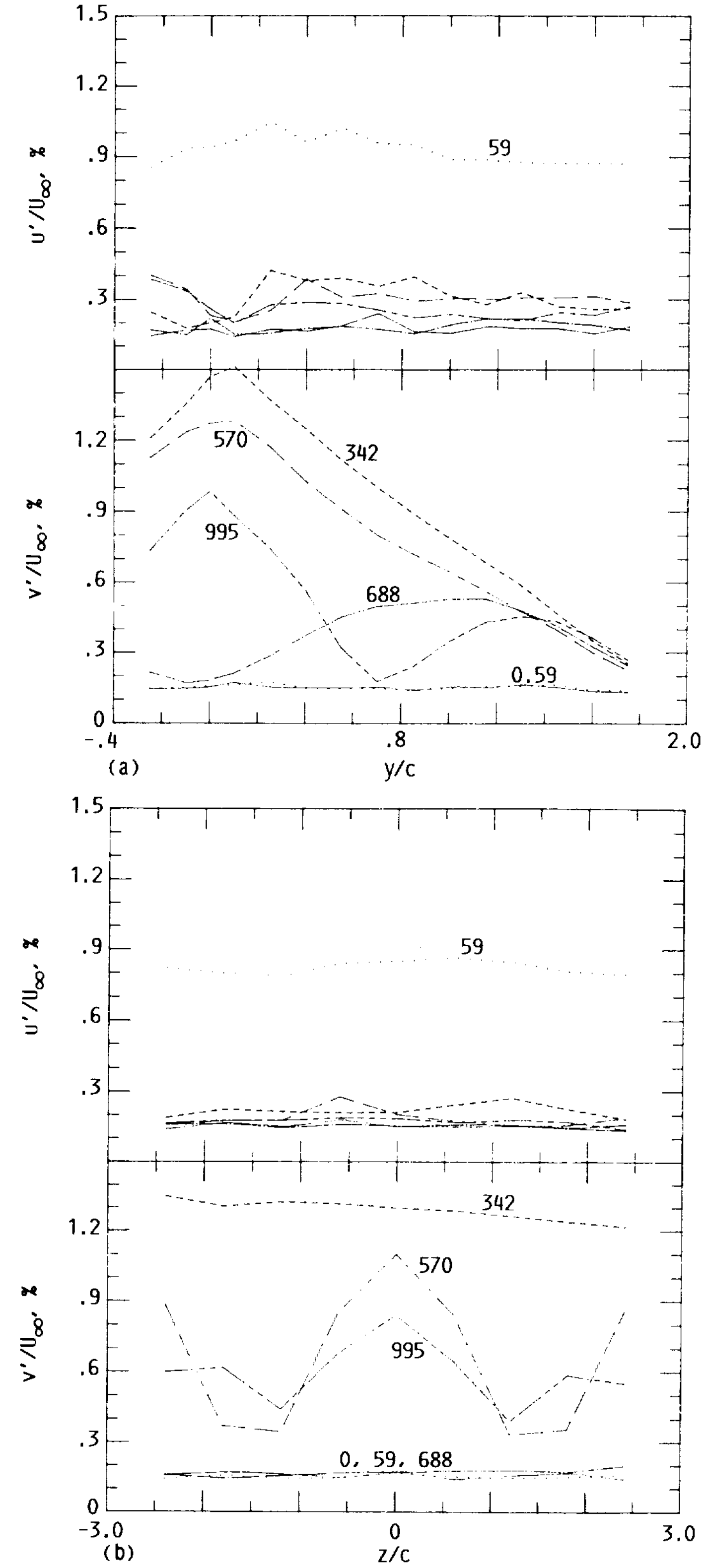

FIG. 6(a) - u' AND v' AMPLITUDES VERSUS y MEASURED AT x = -11.4 cm AND z = 0, FOR INDICATED f_p's. SAME FLOW AS IN FIG. 5. (b) - u' AND v' AMPLITUDES VERSUS z MEASURED AT x = -11.4 cm AND y = 1.27 cm.

ORIGINAL PAGE IS OF POOR QUALITY

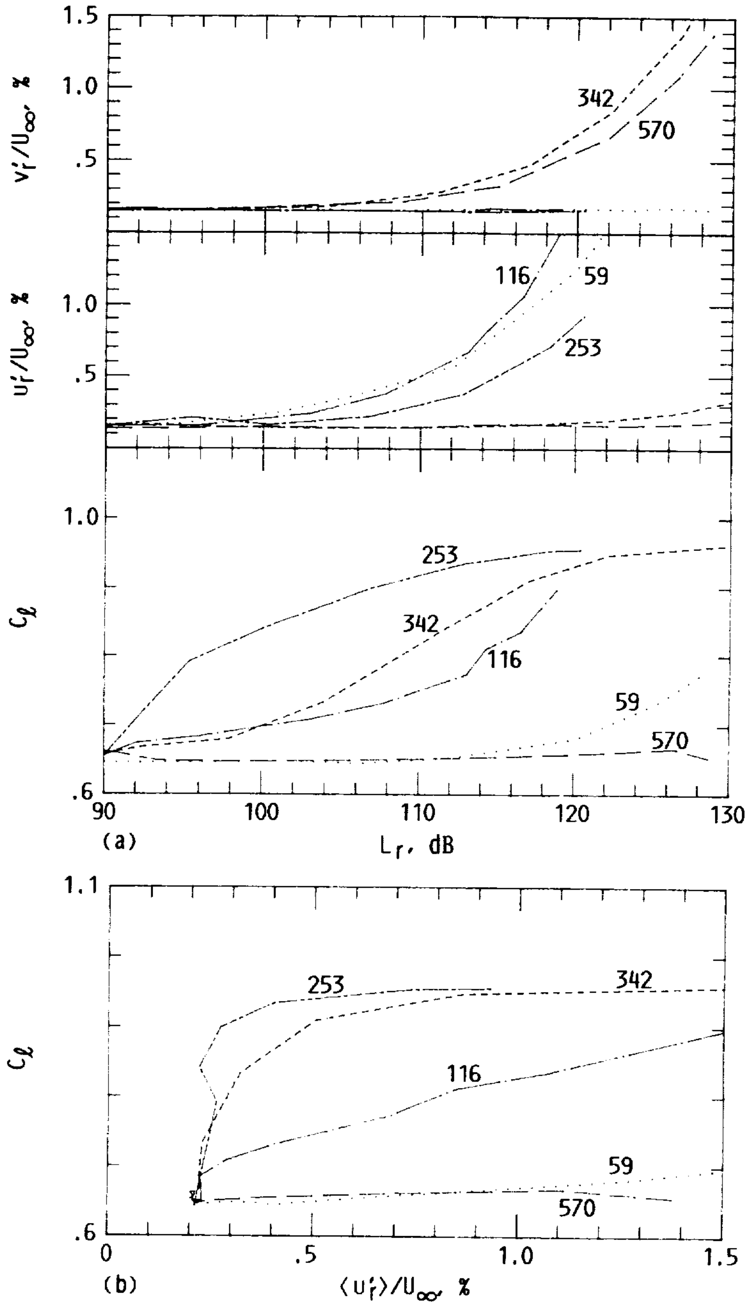

FIG. 7(a) - EXCITATION AMPLITUDE EFFECT ON C_ℓ AT INDICATED f_p's. REFERENCE u_r' AND v_r' VERSUS L_r SHOWN ON TOP. SAME FLOW AS IN FIG. 5.
(b) - C_ℓ DATA OF FIG. 7(a) CROSS PLOTTED AS A FUNCTION OF $\langle u_r' \rangle$.

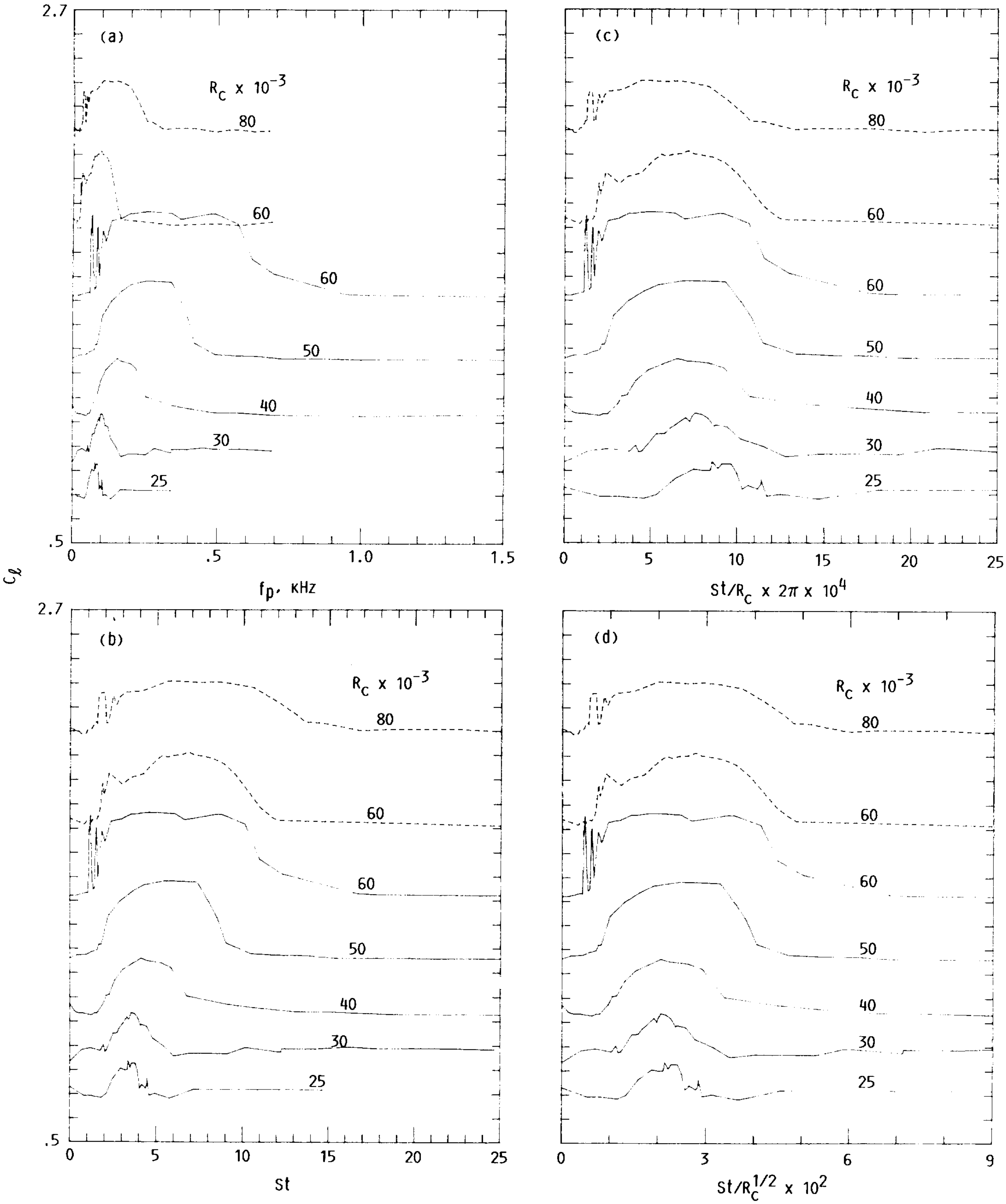

FIG. 8(a) - C_l VERSUS f_p FOR THE LRN AIRFOILS AT $\alpha = 6^0$; $\langle u_r' \rangle / U_\infty = 0.005$. ORDINATE APPLIES TO THE BOTTOM CURVE, OTHERS ARE STAGGERED SUCCESSIVELY BY TWO DIVISIONS. SOLID LINES FOR $c = 12.7$ CM MODEL, DASHED LINES FOR $c = 25.4$ CM MODEL. (b), (c), (d) - DATA REPLOTTED AS A FUNCTION OF INDICATED ABSCISSAE.

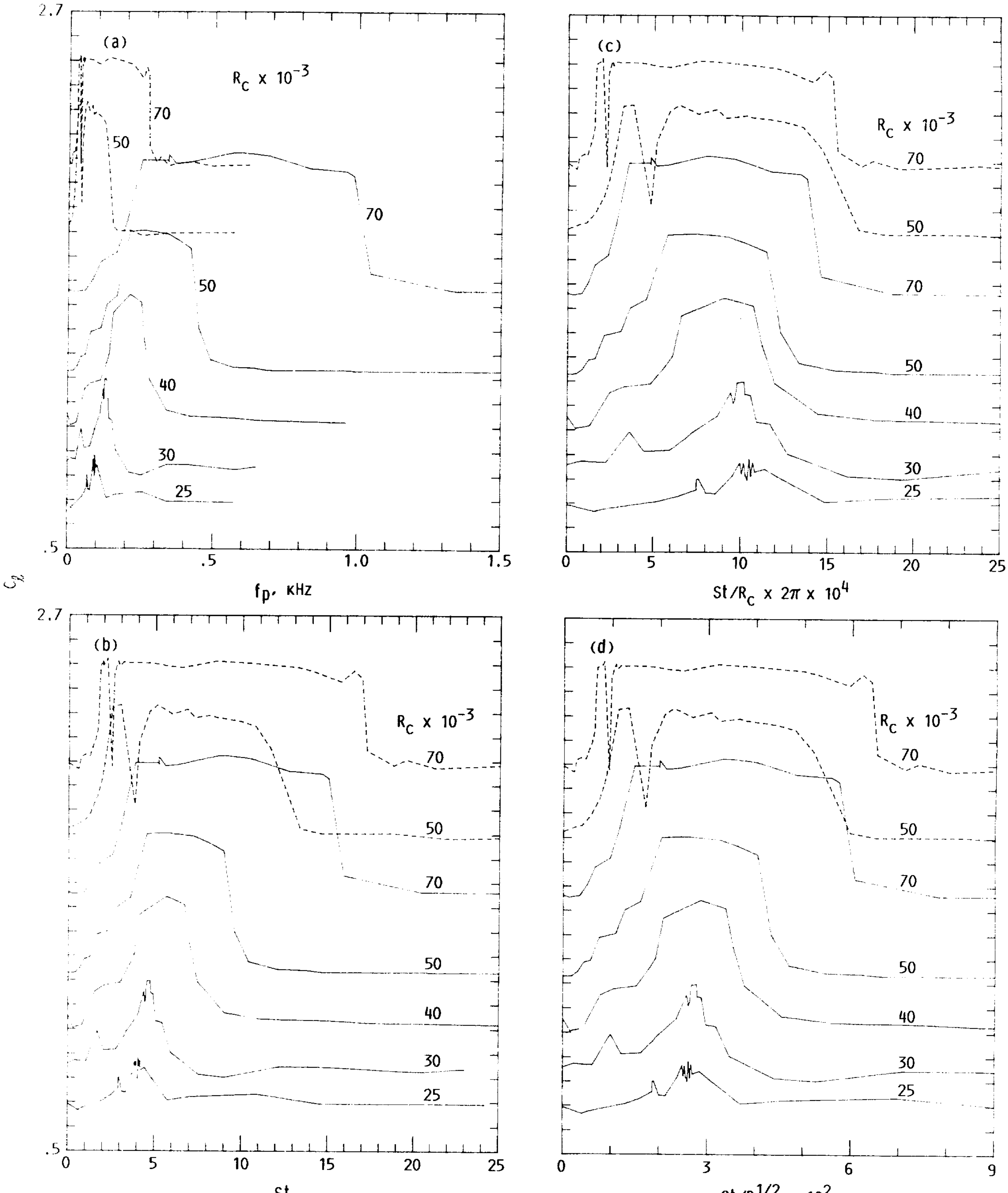

FIG. 9 - C_ℓ VERSUS f_p DATA, AS IN FIG. 8, FOR THE WORTMANN AIRFOILS.

ORIGINAL PAGE IS
OF POOR QUALITY

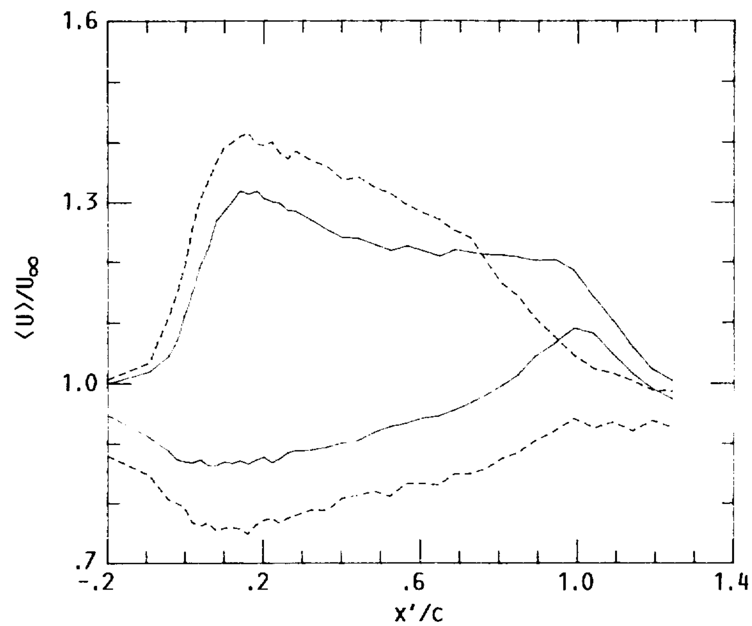

FIG. 10 - ⟨U⟩ VERSUS x' MEASURED AT CONSTANT y; $y = 1.65$ CM FOR THE UPPER TWO CURVES, $y = -1.4$ CM FOR THE LOWER TWO CURVES. SOLID LINE, NO EXCITATION; DASHED LINE, EXCITATION AT $f_p = 253$ Hz WITH $\langle u_r' \rangle / U_\infty = 0.005$. LRN AIRFOIL AT $\alpha = 6^0$, $R_c = 50\ 000$.

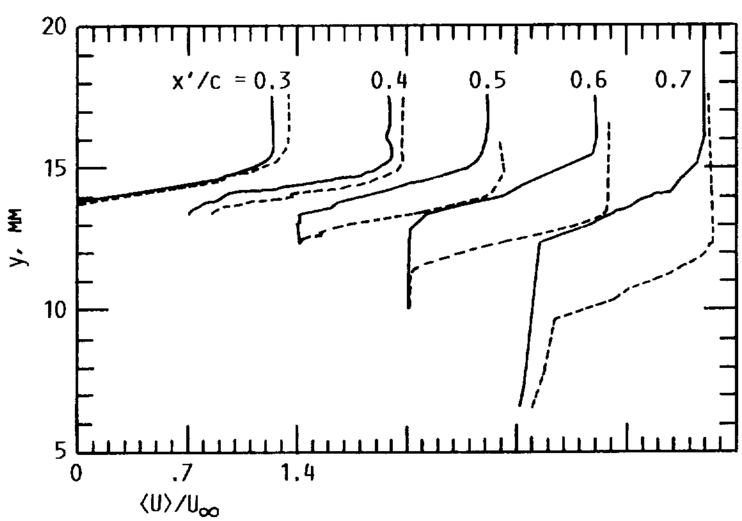

FIG. 11 - BOUNDARY LAYER PROFILES OF ⟨U⟩ AT DIFFERENT x' FOR THE SAME FLOW AS IN FIG. 10. SOLID LINES FOR UNEXCITED FLOW, DASHED LINES FOR EXCITATION AT $f_p = 253$ Hz AND $\langle u_r' \rangle / U_\infty \approx 0.0025$. ABSCISSA APPLIES TO PAIR ON LEFT, OTHERS ARE SHIFTED TO THE RIGHT SUCCESSIVELY BY ONE MAJOR DIVISION.

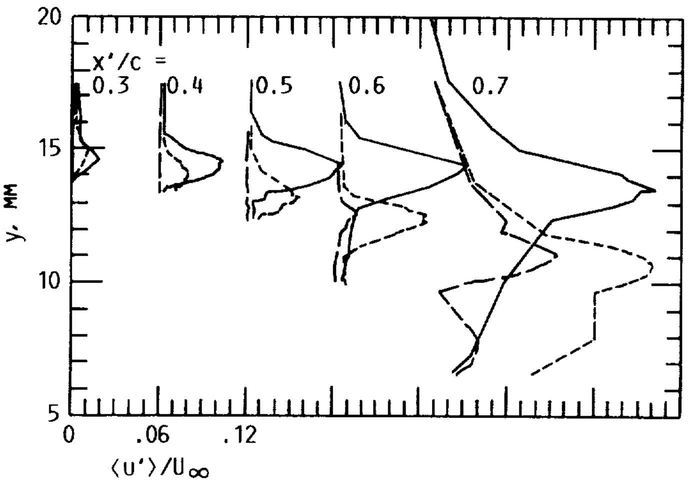

FIG. 12 - R.M.S. AMPLITUDE PROFILES CORRESPONDING TO THE DATA OF FIG. 11. SOLID LINE, TOTAL ⟨u'⟩ FOR THE UNEXCITED FLOW; SHORT DASHED LINE, TOTAL ⟨u'⟩ FOR THE EXCITED FLOW; LONG DASHED LINE, FUNDAMENTAL $\langle u_f' \rangle$ FOR THE EXCITED FLOW. SUCCESSIVE SET OF CURVES SHIFTED TO RIGHT AS IN FIG. 11.

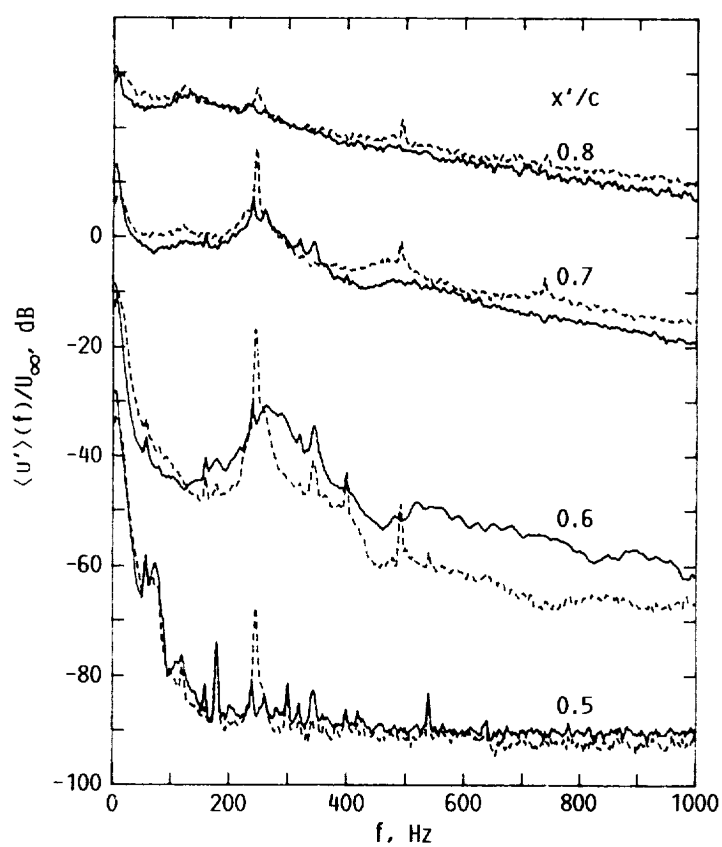

FIG. 13 - ⟨u'⟩-SPECTRA IN THE BOUNDARY LAYER AT 70% VELOCITY POINT. SOLID LINE, FOR UNEXCITED FLOW; DASHED LINE, FOR EXCITATION AT f_p = 253 Hz, $\langle u_f' \rangle/U_\infty \approx 0.0025$. ORDINATE APPLIES TO BOTTOM PAIR, OTHERS STAGGERED SUCCESSIVELY BY TWO DIVISIONS.

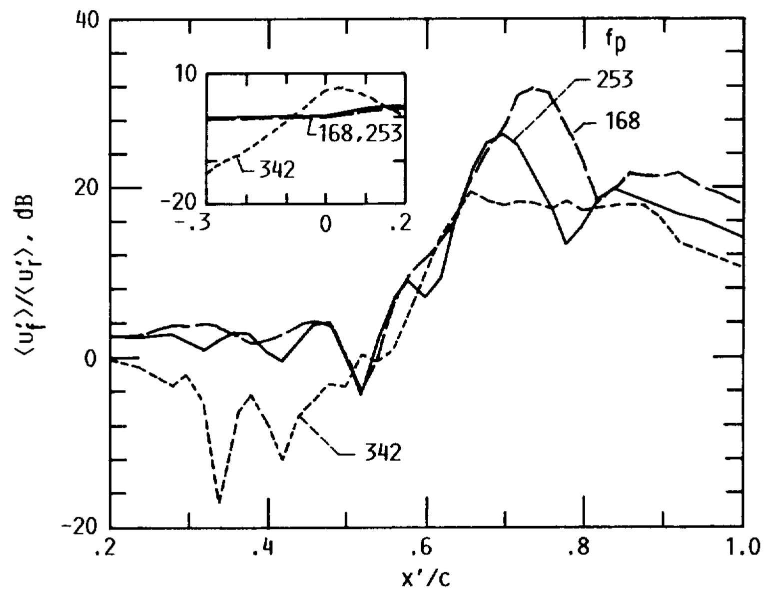

FIG. 14 - $\langle u_f' \rangle$ VERSUS x' MEASURED ALONG 70% VELOCITY POINT ON THE UPPER SURFACE FOR INDICATED f_p's. SAME FLOW AS IN FIG. 10; $\langle u_r' \rangle / U_\infty = 0.005$.

NASA
National Aeronautics and Space Administration

Report Documentation Page

1. Report No.	2. Government Accession No.	3. Recipient's Catalog No.
NASA TM-101379 AIAA-89-0565		

4. Title and Subtitle	5. Report Date
Control of "Laminar Separation" Over Airfoils by Acoustic Excitation	
	6. Performing Organization Code
7. Author(s) K.B.M.Q. Zaman and D.J. McKinzie	8. Performing Organization Report No. E-4434
	10. Work Unit No. 505-62-21
9. Performing Organization Name and Address National Aeronautics and Space Administration Lewis Research Center Cleveland, Ohio 44135-3191	11. Contract or Grant No.
	13. Type of Report and Period Covered Technical Memorandum
12. Sponsoring Agency Name and Address National Aeronautics and Space Administration Washington, D.C. 20546-0001	14. Sponsoring Agency Code

15. Supplementary Notes

Prepared for the 27th Aerospace Sciences Meeting sponsored by the American Institute of Aeronautics and Astronautics, Reno, Nevada, January 9-12, 1989.

16. Abstract

The effect of acoustic excitation in reducing "laminar separation" over two-dimensional airfoils at low angles of attack is investigated experimentally. Airfoils of two different cross sections, each with two different chord lengths, are studied in the chord Reynolds number range of $25\,000 < R_c < 100\,000$. While keeping the amplitude of the excitation induced velocity perturbation a constant, it is found that the most effective frequency scales as $U_\infty^{3/2}$. The parameter $St/R_c^{1/2}$, corresponding to the most effective f_p for all the cases studied, falls in the range of 0.02 to 0.03, St being the Strouhal number based on the chord.

17. Key Words (Suggested by Author(s))	18. Distribution Statement
Airfoils Separation Excitation	Unclassified – Unlimited Subject Category 02

19. Security Classif. (of this report)	20. Security Classif. (of this page)	21. No of pages	22. Price*
Unclassified	Unclassified	18	A03

NASA FORM 1626 OCT 86

*For sale by the National Technical Information Service, Springfield, Virginia 22161

National Aeronautics and
Space Administration

Lewis Research Center
Cleveland, Ohio 44135

Official Business
Penalty for Private Use $300

SECOND CLASS MAIL

ADDRESS CORRECTION REQUESTED

U.S. MAIL

Postage and Fees Paid
National Aeronautics and
Space Administration
NASA-451

NASA